SIViP (2017) 11:769–776
DOI 10.1007/s11760-016-1021-3

ORIGINAL PAPER

Gender classification from facial images using gray relational analysis with novel local binary pattern descriptors

Yılmaz Kaya[1] · **Ömer Faruk Ertuğrul**[2]

Received: 2 May 2016 / Revised: 28 August 2016 / Accepted: 7 November 2016 / Published online: 18 November 2016

Abstract Gender classification (GC) is one of the major tasks in human identification that increase its accuracy. Local binary pattern (LBP) is a texture method that employed successfully. But LBP suffers a major problem; it cannot capture spatial relationships among local textures. Therefore, in order to increase the accuracy of GC, two LBP descriptors, which are based on (1) spatial relations between neighbors with a distance parameter, and (2) spatial relations between a reference pixel and its neighbor on the same orientation, were employed to extract features from facial images. Additionally, gray relational analysis (GRA) was carried out to identify gender through extracted features. Experiments on the FEI database illustrated the effectiveness of the proposed approaches. Achieved accuracies are 97.14, 93.33, and 92.50% by applying GRA with the nLBP_d, dLBP_α, and traditional LBP features, respectively. Experimental results indicated that the proposed approaches were very competitive feature extraction methods in GC. Present work also showed that the nLBP_d, dLBP_α methods were obtained more acceptable results than traditional LBP.

Keywords Local binary patterns · nLBP_d · dLBP_α · Gender classification · Gray relational analysis

✉ Yılmaz Kaya
yilmazkaya1977@gmail.com

[1] Department of Computer Engineering, Siirt University, 56100 Siirt, Turkey

[2] Department of Electrical and Electronics Engineering, Batman University, 72100 Batman, Turkey

1 Introduction

Because of the security purposes, the importance of biometric analysis is increased day by day and human identification is one of them [1–9]. Since detecting the gender of a face decreases the number of possible candidates, gender classification (GC) is a significant stage in human identification, Which means the accuracy of human identification can be increased by employing a successful GC method [10,11]. Therefore, many different GC methods, which can be divided into texture, statistical, and geometry-based methods, were presented [1]. Texture analysis methods are one of the widely employed image processing method and in GC gray-level co-occurrence matrices (GLCM) [12], local binary patterns (LBP) [13,14], Gabor filters (GF), edge histogram, and wavelet methods used successfully [15]. Each of the texture methods is built on detecting different types of textures from an image, and therefore, each of them has its own advantages and disadvantages. LBP [13] is a statistical texture method that focuses on local changes in the image. In LBP, each pixel was compared with its neighbors that are located around it. Later, the results of comparisons (binary patterns), which are a set (totally 8 digits) of 0 or 1 s, were converted to decimal numbers. Finally, the histograms of obtained decimal numbers were used as textures of the image [16,17].

Due to the advantages of LBP such as being less sensitive to changes in illumination of images, requiring less computational cost, being easily implemented [18,19], the LBP was employed in GC systems in various ways. Ahonen et al. [20] employed traditional LBP to face images. Li et al. [2] used it with Adaboost learning to near infrared images. It was also employed with Gabor filters [21]. Mäkinen and Raisamo [22] achieved 80.56% accuracy by traditional LBP and SVM. Sun et al. obtained 95.75% accuracy by LBP and Adaboost classifier [23]. Moreover, Lian and Lu [24]achieved 96.75%

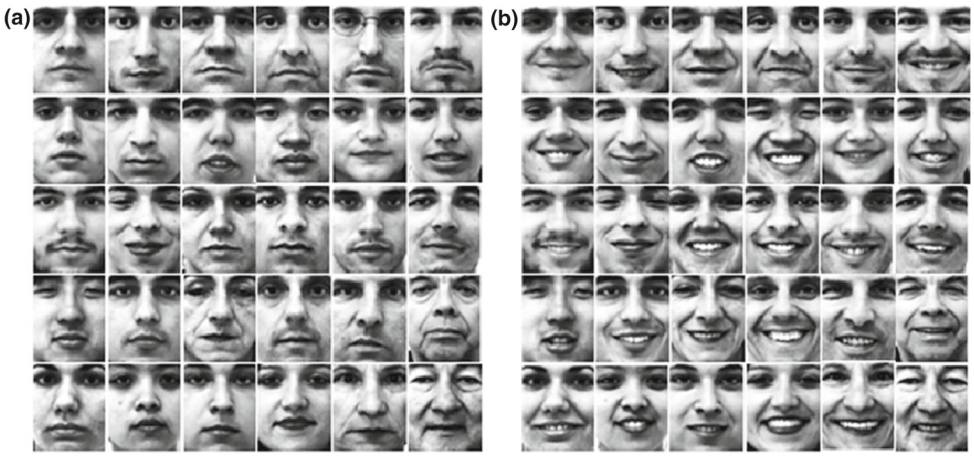

Fig. 1 Examples of FEI face dataset. **a** FEI A: neutral facial images and **b** FEI B: smiling facial images

accuracy by LBP with SVM. Although traditional LBP employed successfully in GC, it suffers from an important disadvantage, which is it cannot capture spatial relationships among local textures [21]. The aim of this research is to investigate the applicability of two distinct spatial based LBP descriptors that were introduced by us [14]. These LBP descriptors were built on detecting the spatial relationships of pixels in different directions or distributions. Therefore, they may be more useful to understand the facial images than traditional LBP.

Identifying the gender of a subject from a single image is often difficult, even for humans and it limits the accuracy of most classifiers [7]. Therefore, in the classification stage, the gray relational analysis (GRA), which was defined as a relational measurement of an attribute in separate sequences based on similarity [25], was employed. Due to having the ability to analyze systems or data sequences with partially unknown parameters, providing reliable analytical results, not requiring any statistical assumption or distribution, and being a simple method to follow, understand and implement, GRA becomes a popular method and there is a large literature about it [26–29]. The characteristic of a GC system is very close to a gray system that is defined as a partially known system (i.e., there is incomplete or insufficient information) [30].

The remaining part of this paper is organized as follows. In Sect. 2, we introduce employee dataset. In Sect. 3, the methodology of the traditional LBP descriptor and employed descriptors, which are local binary patterns by neighborhoods (nLBP_d) and directional local binary patterns (dLBP_α), and GRA. Section 4 consists of the experimental results and discussions. The last section concludes the paper.

2 FEI face dataset

The FEI face database contains the face images of 100 male and 100 female subjects, who are students and staff at FEI, between 19–40 years old with their own appearance, hairstyle, and adorns [31,32]. 14 different images that have different facial expressions were taken from an upright frontal position of each subject, while their profiles were rotated up to about 180°. This dataset contains totally 2800 images, which are 640 × 640 pixels sized colorful with a homogenous white background, while the scale might vary about 10%. In this study, the images that have neutral and smile facial expressions were employed. These image set were named as FEI A and FEI B datasets, respectively, and some of them are illustrated in Fig. 1.

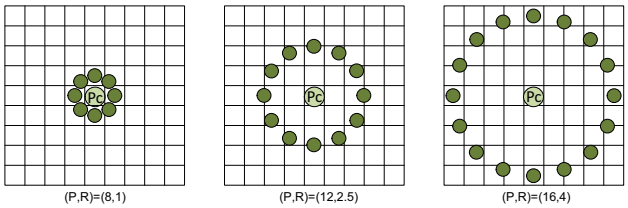

Fig. 2 Neighbors in traditional LBP

3 Methods

3.1 Traditional local binary pattern descriptor

The LBP operator was employed to detect micro patterns in a local region by measuring the local contrast [33]. In LBP descriptor, a binary value was generated for each pixel according to the comparison of the central pixel (P_c) with the value of its neighbors that were around it based on a specific radius as seen in Fig. 2 [13,19,34–36]. LBP has high ability in detecting micro patterns and the change in the radius changes the scale of detectable micropatterns. But, it cannot directly detect large-scale structures. Distinct macropatterns were detected by LBP via micropatterns since macropatterns are compositions of micropatterns [13,14].

As seen in Fig. 2, assigning different radius (R) changes both the positions of neighbor pixels and the total number of

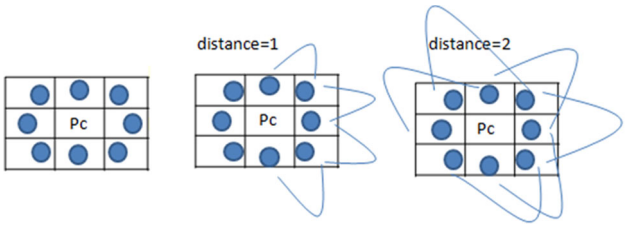

Fig. 3 Spatial comparison between neighbors in the nLBP_d

neighbors (P) that will be compared. Therefore, for each R a distinct pattern will be generated. After determining neighbors of a pixel based on assigned R, a binary value will be calculated based on the comparison between the values of its neighbors with the value of the central pixel. It turns 1 if the central pixel is higher than its neighbor, otherwise, it takes 0. Results of Pcomparisons form a binary number and the histograms of decimal values of obtained binary numbers for each pixel refers to the LBP value of assessed image [13,14].

3.2 Local binary patterns by neighborhoods (nLBP_d)

In nLBP_d, the neighbors are assigned around the central pixel similar to LBP. But, comparisons are done between neighbors instead of the central pixel as shown in Fig. 3 [14]. Each neighbor is compared with its neighbors at distance "d" in clockwise. Later, the same procedure of LBP is employed to determine nLBP_d value of an image

3.3 Directional local binary patterns (dLBP_α)

In dLBP_α, the neighbors were assigned on a straight line with orientation angle (such as 0°, 45°, 90° or 135°) in a counterclockwise according to $+x$axis as in GLCM as given in Fig. 4 [12,14]. The difference between these operators with traditional LBP descriptor is on assigning the neighbors, the other processes are same as traditional LBP. The neighborhood vectors in the horizontal, vertical, and two diagonal orientations, $\alpha = (0°, 45°, 90°$ and $135°)$ are shown in Fig. 4.

3.4 Gray relational analysis

GRA is a machine learning method that is generally employed in order to model or assess gray systems, in which the amount of data is not sufficient for recognizing it [37]. GRA works as follows. First, a reference series $[(X_0 = (x_0(1), x_0(2), x_0(3), \ldots x_0(n)]$are selected for each class based on having maximum gray relational grade. Next, the test series $[(Xj = (xj(1), xj(2), xj(3), \ldots xj(n))]$ were generated from taking one sample from test dataset and taking arbitrary samples in the training dataset in order to compare it with the reference series. Later, selected reference and test series are normalized according to smaller or normal factors that were given

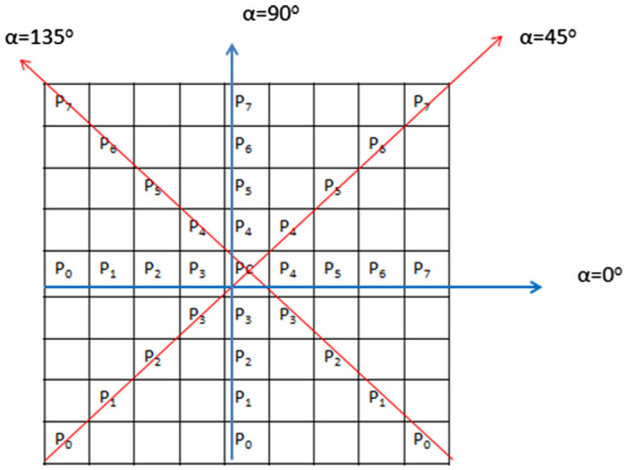

Fig. 4 Neighborhood vectors of dLBP_α

in Eqs. 1 and 2, respectively [29].

$$x_j^{(k)} = \frac{\max\left(x_j^{(k)}\right) - x_{ij}^{(k)}}{\left[\max\left(x_j^{(k)}\right) + \min\left(x_j^{(k)}\right)\right]} \tag{1}$$

$$x_j^{(k)} = 1 - \frac{x_j^{(k)}}{\left[\max\left(x_j^{(k)}\right) + \min\left(x_j^{(k)}\right)\right]} \tag{2}$$

where k indicates criteria index, $x_j^{(k)}$refers series of data, max is the maximum value in the series and min is the minimum value. Next the gray relational coefficient ($\xi_{ij}(k)$) is calculated as follows.

$$\xi_{ij}(k) = \frac{\Delta\min + \rho\Delta\max}{\Delta_{ij}(k) + \rho\Delta\max} \tag{3}$$

where ρ shows the resolution coefficient (it is generally 0.5). $\Delta_{ij}$is the distance between the reference and a test series and calculated by

$$\Delta_{ij}(k) = \left|x_i(k) - x_j(k)\right| \tag{4}$$

Δ min and Δ max refer the minimum absolute difference and the largest absolute difference, respectively. They calculated as follows.

$$\Delta\min = \min_j \min_k \left|x_0(k) - x_j(k)\right| \tag{5}$$

$$\Delta\max = \max_j \max_k \left|x_0(k) - x_j(k)\right| \tag{6}$$

Finally, the gray relational grade (γ_{ij}), which shows the grade of geometric similarity between the two series ($x_j(k)$ and $x_0(k)$), is determined by:

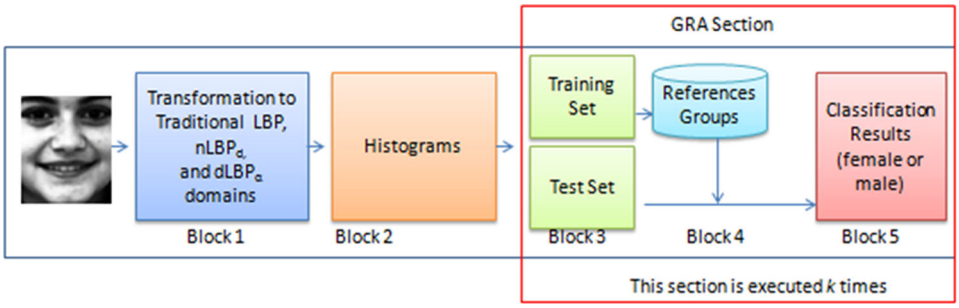

Fig. 5 The block diagram of the employed GC system

$$\gamma_{ij} = \frac{1}{n}\sum_{k=1}^{n}\xi_{ij}(k) \tag{7}$$

Since γ_{ij} is defined as a kind of correlation (similarity) metric between reference series that belongs to each class and test series [29], the class of the sample taken in the test dataset is the same of class that has the higher gray relational grade.

$$\text{Classification} = \begin{cases} \text{Class 1}; & if \quad \gamma_{\text{class1}} < \gamma_{\text{class 2}} \\ \text{Class 2}; & if \quad \gamma_{\text{class1}} >= \gamma_{\text{class 2}} \end{cases} \tag{8}$$

3.5 Employed approach

In this paper, traditional LBP and two LBP descriptors that were introduced by Kaya et al. [14] were employed in GC. The block diagram of the employed approach is displayed in Fig. 5.

Block 1 In the first block, the facial images were transformed into the LBP domain by using traditional LBP, nLBP$_d$, and dLBP$_\alpha$. A decimal value that corresponds to a distinct and a special pattern (its values ranging between 0 and 255), was formed for each pixel by each LBP descriptor. After implementing their procedures, a set of decimal numbers were generated for each image by each LBP descriptor.

Block 2 The histogram of the decimal values of each pixel that were generated by traditional LBP and nLBP$_d$, and dLBP$_\alpha$ descriptors were determined here. LBP histograms were extracted from facial regions as the region-level description, where the n-bin histogram is utilized as a whole. They illustrate how often each of these 256 different patterns appears in its corresponding face image. In order to exact significant and important features from the controlled face images, α parameter in dLBP$_\alpha$ and d parameter in nLBP$_d$ were used for searching effective patterns.

Block 3–5 In the classification stage, the GRA was used to classify the extracted features. Owing to use dissimilar training-test partitions, the algorithm may produce dissimilar results. Therefore, we randomly repeated each analysis for 10 times ($k = 10$), and the mean of obtained results are provided. In the classification process, a template-matching approach was employed.

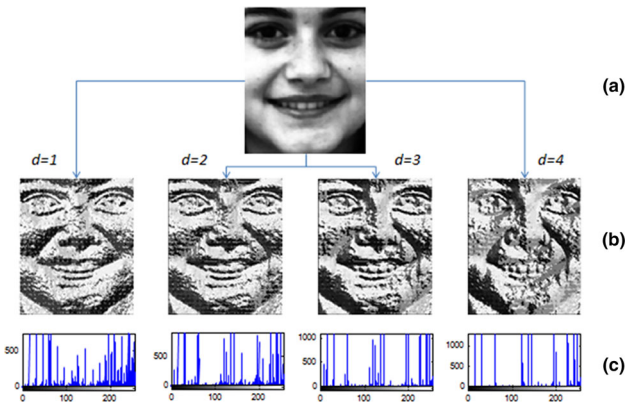

Fig. 6 A sample face images from FEI database. **a** original images, **b** nLBP$_{d=1}$, nLBP$_{d=2}$, nLBP$_{d=3}$ and nLBP$_{d=4}$ images and **c** histograms of nLBP for different distances

4 Results and discussion

Experiments conducted on cropped gray-colored images, and images scaled to size of 162 × 193 pixels. We manually labeled ground truth regarding gender for each face. The features, which extracted by nLBP$_d$ for different distances ($d = 1$–7), dLBP$_\alpha$ in different angles ($\alpha = 0°$–$135°$) and traditional LBP, were classified by GRA. All of these experiments were replicated 10 times with different random partitions (train and test partitions) of the data. The final results were reported as the mean, worst, and best of the results from individual runs.

4.1 Results obtained by nLBP$_d$ descriptor

A sample of obtaining histograms from the FEI face image datasets with different distance values is illustrated in Fig. 6.

As seen in this figure, employing nLBP$_d$ descriptor with different distances both obtained images and their histograms were changed. To determine the optimal distance, both neutral and smile face images were assessed by different distances (d=1–7) and the accuracies obtained by GRA in these trials by nLBP$_d$ are listed in Table 1.

As seen in Table 1 and Fig. 7, different accuracies were obtained while employing different distance parameters. It

Table 1 Obtained GC accuracies (%) by $nLBP_d$ according to different distances

D	Data Set	Neutral facial images					Smile facial images				
	training-test partition	30–70%	40–60%	50–50%	60–40%	70–30%	30–70%	40–60%	50–50%	60–40%	70–30%
1	Min	75.00	72.50	74.00	75.00	73.33	70.00	71.67	72.00	73.75	71.67
	Max	85.00	84.17	87.00	86.25	86.67	84.29	84.17	86.00	86.25	88.33
	Mean	78.79	78.92	78.90	79.37	80.83	77.36	79.25	76.00	79.25	80.50
2	Min	79.29	78.33	79.00	71.25	75.00	70.00	71.67	73.00	72.50	76.67
	Max	87.14	87.50	88.00	88.75	88.33	91.43	90.83	89.00	87.50	91.67
	Mean	82.71	82.42	83.00	81.00	82.33	81.00	80.08	80.40	82.62	81.33
3	Min	71.43	74.17	72.00	75.00	71.67	64.29	66.67	69.00	67.50	70.00
	Max	86.43	89.17	89.00	90.00	91.67	82.86	86.67	85.00	85.00	95.00
	Mean	78.93	80.67	80.30	80.50	80.67	72.00	76.75	76.40	75.50	77.00
4	Min	77.14	70.83	76.00	78.75	85.00	70.00	74.17	74.00	76.25	78.33
	Max	**97.14**	92.50	96.00	96.25	**96.67**	95.71	**96.67**	96.00	96.25	**96.67**
	Mean	82.71	84.00	84.10	87.75	90.17	82.93	82.08	88.30	90.00	87.17
5	Min	74.29	65.83	69.00	68.75	70.00	66.43	67.50	76.00	71.25	66.67
	Max	87.14	83.33	82.00	83.75	86.67	82.86	82.50	81.00	88.75	85.00
	Mean	79.36	76.42	77.50	76.38	78.17	75.79	77.17	78.60	78.63	77.50
6	Min	74.29	76.67	75.00	76.25	73.33	71.43	72.50	67.00	62.50	65.00
	Max	87.14	89.17	85.00	86.25	88.33	83.57	81.67	85.00	87.50	88.33
	Mean	81.36	82.83	80.60	81.75	82.17	77.64	74.83	76.10	77.25	74.50
7	Min	73.57	74.17	72.00	73.75	70.00	72.14	75.00	74.00	75.00	75.00
	Max	85.00	83.33	87.00	83.75	81.67	88.57	85.83	84.00	85.00	85.00
	Mean	79.43	79.33	78.80	78.88	77.50	77.71	77.67	79.00	79.13	78.67

Obtained highest values were given in bold

can be seen that the GRA of the $nLBP_{d=4}$ features gets the highest accuracy, which is 97.14 and 96.67% on the two data sets (smiling and neutral faces). Achieving nearly similar accuracies while using both smaller and larger training datasets showed that the employed approach is robust. Additionally, the employed approach can be successfully used in the areas that large datasets cannot be generated.

4.2 Results obtained by $dLBP_\alpha$ descriptor

The obtaining histogram process for different orientations for an image in FEI face database is demonstrated in Fig. 7.

As seen in this figure, the optimum orientation can only be determined by trials or experience. Obtained GC accuracies by GRA using the features extracted by $dLBP_\alpha$ with different orientations are summarized in Table 2.

As seen in Table 2, the highest accuracies obtained for two datasets are 93.33% ($dLBP_{\alpha=45^\circ}$) and 88.57% ($dLBP_{\alpha=45^\circ}$). That means the micropatterns that were obtained through a line with 45° orientation have a higher power in distinguishing face images. This may be because of the characteristics of the faces. Additionally, these results showed that obtained accuracies are strongly related to the selected orientations.

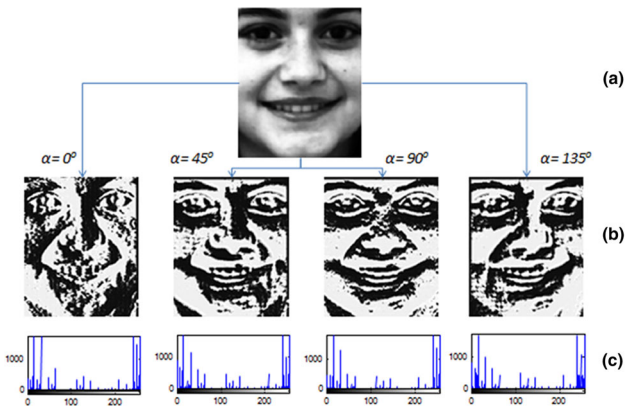

Fig. 7 A sample face image from FEI database. **a** original images, **b** $dLBP_{\alpha=0}$, $dLBP_{\alpha=45}$, $dLBP_{\alpha=90^\circ}$ and $dLBP_{\alpha=135^\circ}$ images and **c** histograms of $dLBP_\alpha$ for different orientations

4.3 Comparison of $nLBP_d$, $aLBP_\alpha$, and traditional LBP operators

Accuracies obtained by employed LBP operators (traditional LBP, $nLBP_d$, and $dLBP_\alpha$) are summarized in Table 3.

As it is clear from Table 3 that $nLBP_d$ and $dLBP_\alpha$ descriptors showed higher accuracies than traditional LBP. The

Table 2 Obtained GC accuracies (%) by $dLBP_{\alpha}$ according to different orientations

Data sets	Training-test partition	$\alpha = 0°$			$\alpha = 45°$			$\alpha = 90°$			$\alpha = 135°$		
		Min	Max	Mean	Min	Max	Mean	Min	Max	Mean	Min	Max	Mean
Neutral facial images	30–70%	74.29	82.86	78.86	72.86	82.14	78.43	71.43	84.29	77.29	70.00	82.14	76.14
	40–60%	76.67	86.67	81.50	74.17	84.17	80.25	73.33	84.17	77.17	70.00	85.00	78.50
	50–50%	73.00	89.00	81.70	78.00	88.00	81.90	73.00	87.00	78.40	73.00	87.00	78.00
	60–40%	76.25	88.75	81.38	77.50	88.75	83.37	73.75	87.50	80.13	73.75	88.75	80.63
	70–30%	76.67	88.33	81.50	75.00	**93.33**	82.83	71.67	88.33	77.50	70.00	88.33	76.67
Smile facial images	30–70%	73.57	79.29	76.43	68.57	**88.57**	75.29	67.14	86.43	76.57	67.14	81.43	73.21
	40–60%	73.33	80.83	77.25	67.50	84.17	76.08	71.67	89.17	77.75	71.67	82.50	74.83
	50–50%	70.00	81.00	76.70	68.00	83.00	76.20	72.00	87.00	79.20	68.00	82.00	75.00
	60–40%	72.50	83.75	77.50	67.50	87.50	76.12	72.50	88.75	78.13	67.50	82.50	74.62
	70–30%	71.67	83.33	76.67	73.33	88.33	78.83	73.33	88.33	79.00	66.67	83.33	73.83

Obtained highest values were given in bold

Table 3 GC accuracies (%) obtained by employing traditional LBP, $nLBP_{d}$ and $dLBP_{\alpha}$ descriptors

Data sets	Training-test partition	LBP			$nLBP_{d=4}$			$aLBP_{\alpha=45°}$		
		Min	Max	Mean	Min	Max	Mean	Min	Max	Mean
Neutral facial images	30–70%	70.00	86.43	80.93	77.14	**97.14**	82.71	72.86	82.14	78.43
	40–60%	77.50	90.00	82.50	70.83	92.50	84.00	74.17	84.17	80.25
	50–50%	74.00	88.00	82.30	76.00	96.00	84.10	78.00	88.00	81.90
	60–40%	77.50	**92.50**	84.38	78.75	96.25	87.75	77.50	88.75	83.37
	70–30%	76.67	91.67	83.50	85.00	96.67	90.17	75.00	**93.33**	82.83
Smile facial images	30–70%	72.86	85.71	80.14	70.00	95.71	82.93	68.57	**88.57**	75.29
	40–60%	75.00	85.00	79.83	74.17	**96.67**	82.08	67.50	84.17	76.08
	50–50%	73.00	85.00	78.60	74.00	96.00	88.30	68.00	83.00	76.20
	60–40%	73.75	83.75	78.13	76.25	96.25	90.00	67.50	87.50	76.12
	70–30%	71.67	**86.67**	79.50	78.33	**96.67**	87.17	73.33	88.33	78.83

Obtained highest values were given in bold

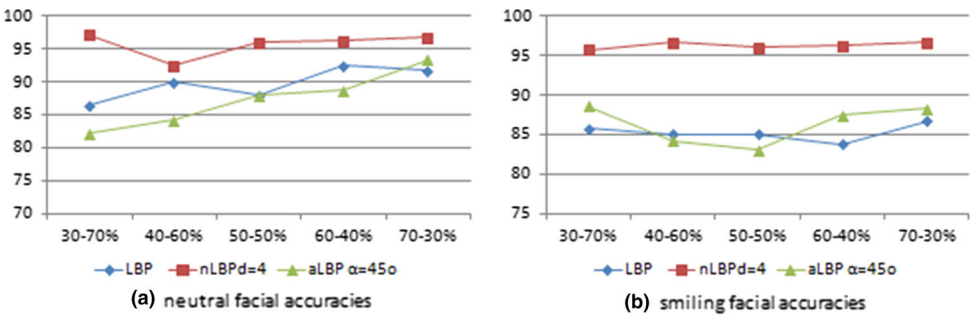

Fig. 8 Classification rates (CR) of $nLBP_{d=4}$, $dLBP_{\alpha=45°}$ and traditional LBP methods. **a** CR for neutral facial images. **b** CR for smiling facial images

highest accuracy of FEI face database is obtained, while using $nLBP_{d=4}$ and $dLBP_{\alpha=45°}$ descriptors. For the first experiment the highest accuracy is 97.14% by using $nLBP_{d=4}$ features, for 30–70% training-test partition. For the second experiment, 96.67% accuracy was obtained for 40–60% and 70–30% to 96.67% training-test partition sets. Figure 8 shows the classification rates of $nLBP_{d=4}$ $dLBP_{\alpha=45°}$ and traditional LBP features with GRA for all training-test partitions.

Table 4 Comparison of recent studies on GC

References	Dataset	Features	Classifier	Classification rate (%)
Rai and Khanna [3]	FEI	Gabor features and 2D PCA	SVM	97.10
Shan [5]	LFW	Boosted LBP features	SVM	94.81
Mäkinen and Raisamo [22]	FERET	LBP	SVM	92.86
Sun et al. [23]	FERET	LBP	Adaboost	95.75
BenAbdelkader and Griffin [38]	–	Local region matching	SVM	94.20
Hadid and Pietikäinen [39]	MoBo	LBP features	SVM	91.00
Berbar [40]	FERET	GLCM	SVM	93.11
Zheng and Lu [41]	FERET	LGBP, MLBP, LBP	SVMAC	96.40
Andreu and Mollineda [42]	FERET	Gray-level linear vector with PCA	SVM	95.00
This study	FEI	$nLBP_d$	GRA	97.14
		$dLBP_\alpha$		96.67

4.4 Recent studies in GC

Recent studies in GC ARE summarized in Table 4 in order to validate the performance of employed $nLBP_d$ and $dLBP_\alpha$ descriptors.

It can be seen in Table 4 that, employed approach could produce significant performance compared to other studies in the literature. Achieved high accuracies may be because of employed LBP descriptors that can detect different spatial patterns or GRA, which is a successful classification tool for gray systems or data.

5 Conclusions

Human faces provide important visual information in GC that may be employed as a preprocessing stage in human identification. GC from face images has received much research interest in the last two decades. Although traditional LBP operator has a high ability in detecting micro patterns and showed high accuracy in various image processing applications, it can only search patterns that have a specific neighborhood. Therefore, some versions of LBP, which can detect special patterns, have been presented. In this paper, we employed two LBP descriptors and GRA from facial images in order to achieve higher accuracies in GC. The first LBP descriptor ($nLBP_d$) is based on the relations between the sequential neighbors and the other one ($dLBP_\alpha$) is based on determining the neighbors in the same orientation. Because of taking into account the spatial relationships between pixels, higher accuracies in GC were obtained by both $nLBP_d$ and $dLBP_\alpha$ descriptors with compared to results obtained by traditional LBP and results reported in the literature.

References

1. Shih, H.C.: Robust gender classification using a precise patch histogram. Pattern Recognit. **46**(2), 519–528 (2013)
2. Li, B., Lian, X.C., Lu, B.L.: Gender classification by combining clothing, hair and facial component classifiers. Neurocomputing **76**(1), 18–27 (2012)
3. Rai, P., Khanna, P.: A gender classification system robust to occlusion using Gabor features based (2D) 2 PCA. J. Vis. Commun. Image Represent. **25**(5), 1118–1129 (2014)
4. Andreu, Y., García-Sevilla, P., Mollineda, R.A.: Face gender classification: a statistical study when neutral and distorted faces are combined for training and testing purposes. Image Vis. Comput. **32**(1), 27–36 (2014)
5. Shan, C.: Learning local binary patterns for gender classification on real-world face images. Pattern Recognit. Lett. **33**(4), 431–437 (2012)
6. Xia, B., Amor, B.B., Drira, H., Daoudi, M., Ballihi, L.: Combining face averageness and symmetry for 3D-based gender classification. Pattern Recognit. **48**(3), 746–758 (2015)
7. Chu, W.S., Huang, C.R., Chen, C.S.: Gender classification from unaligned facial images using support subspaces. Inf. Sci. **221**, 98–109 (2013)
8. Eskandari, M., Toygar, Ö., Demirel, H.: Feature extractor selection for face-iris multimodal recognition. Signal Image Video Process. **8**(6), 1189–1198 (2014)
9. Hadid, A., Dugelay, J.L., Pietikäinen, M.: On the use of dynamic features in face biometrics: recent advances and challenges. Signal Image Video Process. **5**(4), 495–506 (2011)
10. Jain, A., Huang, J.: Integrating independent components and linear discriminant analysis for gender classification. In: Proceedings Sixth IEEE International Conference on Automatic Face and Gesture Recognition, 2004, IEEE, pp. 159–163. (2004)
11. Daneshmand, M., Aabloo, A., Ozcinar, C., Anbarjafari, G.: Real-time, automatic shape-changing robot adjustment and gender classification. Signal Image Video Process. **10**(4), 753–760 (2016)
12. Haralick, R.M., Shanmugam, K., Dinstein, I.H.: Textural features for image classification. IEEE Trans. Syst. Man Cybern. **6**, 610–621 (1973)
13. Ojala, T., Pietikäinen, M., Harwood, D.: A comparative study of texture measures with classification based on featured distributions. Pattern Recognit. **29**(1), 51–59 (1996)
14. Kaya, Y., Ertuğrul, Ö.F., Tekin, R.: Two novel local binary pattern descriptors for texture analysis. Appl. Soft Comput. **34**, 728–735 (2015)
15. Bozkurt, A., Duygulu, P., Cetin, A.E.: Classifying fonts and calligraphy styles using complex wavelet transform. Signal Image Video Process. **9**(1), 225–234 (2015)

16. Zhou, H., Wang, R., Wang, C.: A novel extended local-binary-pattern operator for texture analysis. Inf. Sci. **178**(22), 4314–4325 (2008)
17. Fathi, A., Naghsh-Nilchi, A.R.: Noise tolerant local binary pattern operator for efficient texture analysis. Pattern Recognit. Lett. **33**(9), 1093–1100 (2012)
18. Nanni, L., Brahnam, S., Lumini, A.: A simple method for improving local binary patterns by considering non-uniform patterns. Pattern Recognit. **45**(10), 3844–3852 (2012)
19. Nosaka, R., Fukui, K.: Hep-2 cell classification using rotation invariant co-occurrence among local binary patterns. Pattern Recognit. **47**(7), 2428–2436 (2014)
20. Ahonen, T., Hadid, A., Pietikainen, M.: Face description with local binary patterns: application to face recognition. IEEE Trans. Pattern Anal. Mach. Intell. **28**(12), 2037–2041 (2006)
21. Nirmala, S., Nagabhushan, P.: Foreground text segmentation in complex color document images using Gabor filters. Signal Image Video Process. **6**(4), 669–678 (2012)
22. Mäkinen, E., Raisamo, R.: An experimental comparison of gender classification methods. Pattern Recognit. Lett. **29**(10), 1544–1556 (2008)
23. Sun, N., Zheng, W., Sun, C., Zou, C., Zhao, L.: Gender classification based on boosting local binary pattern. In: Advances in Neural Networks-ISNN 2006, pp. 194–201. Springer (2006)
24. Lian, X.C., Lu, B.L.: Gender classification by combining facial and hair information. In: Advances in Neuro-Information Processing, pp. 647–654. Springer (2009)
25. Chang, W.C.: A comprehensive study of grey relational generating. J. Grey Syst. **3**(3), 53–57 (2000)
26. Kayacan, E., Ulutas, B., Kaynak, O.: Grey system theory-based models in time series prediction. Expert Syst. Appl. **37**(2), 1784–1789 (2010)
27. Liu, S., Lin, Y.: An introduction to grey systems: foundations, methodology and applications, pp. 120–155. IIGSS Academic Publisher, Slippery Rock (1998)
28. Hsiao, S.W., Tsai, H.C.: Use of gray system theory in product-color planning. Color Res. Appl. **29**(3), 222–231 (2004)
29. Lin, Y.H., Lee, P.C., Chang, T.P.: Practical expert diagnosis model based on the grey relational analysis technique. Expert Syst. Appl. **36**(2), 1523–1528 (2009)
30. Lin, Y., Liu, S.: A historical introduction to grey systems theory. In: Proceedings of IEEE International Conference on Systems, Man and Cybernetics, The Netherlands, vol. 3, pp. 2403–2408 (2004)
31. Thomaz, C.E., Giraldi, G.A.: A new ranking method for principal components analysis and its application to face image analysis. Image Vis. Comput. **28**(6), 902–913 (2010)
32. Moin, M.S., Sepas-Moghaddam, A.: Face recognition in JPEG compressed domain: a novel coefficient selection approach. Signal Image Video Process. **9**(3), 651–663 (2015)
33. Ojala, T., Pietikäinen, M., Mäenpää, T.: Multiresolution gray-scale and rotation invariant texture classification with local binary patterns. IEEE Trans. Pattern Anal. Mach. Intell. **24**(7), 971–987 (2002)
34. Kaya, Y., Kayci, L., Tekin, R., Faruk Ertuğrul, Ö.: Evaluation of texture features for automatic detecting butterfly species using extreme learning machine. J. Exp. Theor. Artif. Intell. **26**(2), 267–281 (2014)
35. Burçin, K., Vasif, N.V.: Down syndrome recognition using local binary patterns and statistical evaluation of the system. Expert Syst. Appl. **38**(7), 8690–8695 (2011)
36. Gerek, O.N., Cetin, A.E., Tewfik, A.H., Atalay, V.: Subband domain coding of binary textual images for document archiving. IEEE Trans. Image Process. **8**(10), 1438–1446 (1999)
37. Deng, J.L.: Introduction to grey system theory. J. Grey Syst. **1**, 1–24 (1989)
38. BenAbdelkader, C., Griffin, P.: A local region-based approach to gender classification from face images. In: IEEE Computer Society Conference on Computer Vision and Pattern Recognition-Workshops, 2005. CVPR Workshops, IEEE, pp. 52–52. (2005)
39. Hadid, A., Pietikäinen, M.: Combining appearance and motion for face and gender recognition from videos. Pattern Recognit. **42**(11), 2818–2827 (2009)
40. Berbar, M.A.: Three robust features extraction approaches for facial gender classification. Vis. Comput. **30**(1), 19–31 (2014)
41. Zheng, J., Lu, B.L.: A support vector machine classifier with automatic confidence and its application to gender classification. Neurocomputing **74**(11), 1926–1935 (2011)
42. Andreu, Y., Mollineda, R.A. : On the complementarity of face parts for gender recognition. In: Progress in Pattern Recognition, Image Analysis and Applications, pp. 252–260. Springer (2008)